Rapid Extraction of Urban Road Guardrails From Mobile LiDAR Point Clouds

Jianlan Gao, Yiping Chen, *Senior Member, IEEE*, José Marcato Junior, *Member, IEEE*, Cheng Wang, *Senior Member, IEEE*, and Jonathan Li, *Senior Member, IEEE*

***Abstract*— Mobile Laser Scanning (MLS) systems provide highly dense 3D point clouds that enable the acquisition of accurate traffic facilities information for intelligent transportation system. Road guardrails with safety features that can separate traffic and define moving spaces for pedestrians and vehicles face challenges such as diverse guardrail types and continuous slopes in point clouds data. This paper proposes a novel approach for rapidly extracting urban road guardrails from MLS point clouds, combining a proposed multi-level filtering with a modified Density-Based Spatial Clustering of Applications with Noise (DBSCAN) clustering, and adapting for most types of guardrails and rough slope roads. We develop a multi-level filter to detect the road surface and remove the undesirable points. Through a proposed modified DBSCAN clustering, the guardrails are extracted after a four-step screening, which includes the limits based on the number of points, the fitting error, the bounding box size and the average reflection intensity for each cluster. The proposed method achieves high precisions of 97.2% and 96.4% respectively for the lane-separating guardrails and the anti-fall guardrails on the dataset. Extensive experiments with test dataset captured by a RIEGL VMX-450 MLS, show that our method outperforms the state-of-the-art method to extract 3D guardrails from point clouds.**

***Index Terms*— Light detection and ranging, mobile laser scanning, object extraction, point clouds, road guardrails.**

I. Introduction

MOBILE LiDAR point clouds provide rich geometric details of traffic objects with high precision, high density, high collection efficiency, and flexible data acquisition. Rapid extraction of guardrails from mobile LiDAR point clouds conducive to facilitate road asset inventory, basic geographic information update, and road facilities management and maintenance. In addition to the function of indication and distinction, there is a high probability of frequent traffic accidents in locations with guardrails. Hence, it is more crucial and higher security level than the road lines. The main challenge of road guardrails extraction from point clouds is commonality due to the diversity of guardrail types and the uneven roads. Fig. 1 shows several typical guardrails on urban roads.

Researchers working on object detection and classification in point clouds have made great progress in feature learning, real-time performance and accuracy improvement [1]–[3]. Many types of man-made road objects are targeted, such as traffic signs [4], [5], street light poles [6], [7] and vehicles [8], [9]. Relatively few studies have focused on guardrails which show great diversity in shape and form. The existing methods of guardrails detection consist of image-based methods [10], [11], point clouds based methods [12]–[14] and both [15]. The image-based method [10] extracted the objects quickly but had requirements on the position of the guardrails in the image, which led to partly extraction of the guardrails. [11] only worked in the daytime due to the signal noise of the camera in the dark and the sensitivity of the local binary patterns. [12]–[14] were only applicable to one certain type of guardrails. The method [15] did not make full use of the information provided by point clouds, and the training and learning of CNN was only carried out on the image.

Fig. 1. Guardrails on urban roads (the lane-separating guardrails on the left and the anti-fall guardrails on the right).

Few efforts focused on the clustering analysis of point clouds for road guardrail extraction. Our proposed method adapts to different types of guardrails and rough slope roads. The guardrails extraction algorithm from MLS point clouds through the combination of a multi-level filter and a modified Density-Based Spatial Clustering of Applications with Noise (DBSCAN) [16] clustering. The main contributions of this paper are summarized as follows: (1) presenting an extraction framework which is the first one that can simultaneously target diversity types of guardrails in MLS point clouds; (2) exploring a block-based multi-level filter that greatly simplify the complicated road scene point clouds to facilitate the extraction as well as other road targets extraction with similar characteristics as guardrails; (3) exploring a modified DBSCAN clustering to extract different types of guardrails through a cluster-based four-step screening utilizing the general characteristics of guardrails.

The paper is organized as follows. The proposed framework is described in Section II and experiment is in Section III. Section IV presents the conclusion and future directions.

II. Proposed Framework

The proposed method comprises two components for guardrails extraction. (1) Through a multi-level filter, the input MLS point clouds are first preprocessed of subsampling and being cut into near-road blocks; road surface points and undesirable points are then removed using RANdom SAmple Consensus (RANSAC) [17]. (2) Through a modified DBSCAN clustering that contains a four-step screening, the remaining candidate point clouds are clustered, screened and segmented into individual guardrail objects. The pseudocode of the proposed framework is given in Algorithm 1. We elaborate the proposed framework through Fig. 2 which shows the detailed workflow of the entire extraction process.

A. Multi-Level Filtering

1) Preprocessing: The preprocessing contains three steps: subsampling the large-scale point clouds scenes, removing the higher

Manuscript received February 2, 2020; revised June 30, 2020 and August 16, 2020; accepted September 8, 2020. Date of publication September 29, 2020; date of current version February 2, 2022. This work was supported by the National Natural Science Foundation of China under Grant 41871380. The Associate Editor for this article was L. M. Bergasa. *(Corresponding authors: Yiping Chen; Jonathan Li.)*

Jianlan Gao, Yiping Chen, and Cheng Wang are with the Fujian Key Laboratory of Sensing and Computing for Smart Cities, School of Informatics, Xiamen University, Xiamen 361005, China (e-mail: 23320171153180@stu.xmu.edu.cn; chenyiping@xmu.edu.cn; cwang@xmu.edu.cn).

José Marcato Junior is with the Faculty of Engineering, Architecture, Urbanism and Geography, Federal University of Mato Grosso do Sul, Campo Grande 79070-900, Brazil (e-mail: jose.marcato@ufms.br).

Jonathan Li is with the Fujian Key Laboratory of Sensing and Computing for Smart Cities, School of Informatics, Xiamen University, Xiamen 361005, China, and also with the Department of Geography and Environmental Management, University of Waterloo, Waterloo ON N2L 3G1, Canada (e-mail: junli@xmu.edu.cn).

Digital Object Identifier 10.1109/TITS.2020.3025067

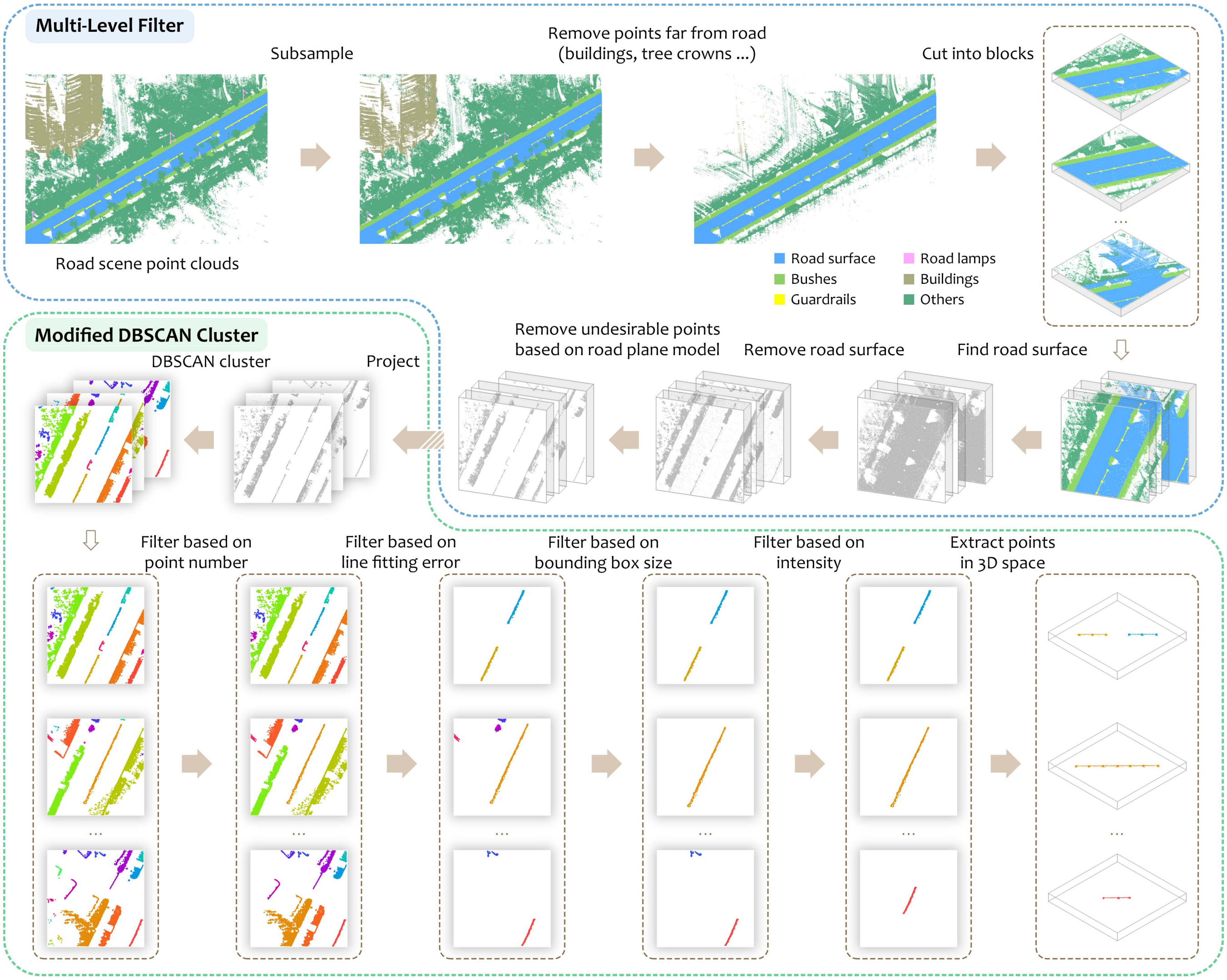

Fig. 2. Workflow of road guardrails extraction. The extraction process is completed in two stages which are separated by blue and green. For easy observation, the road scene point clouds in the first stage are roughly colored to distinguish road surface, guardrails, bushes, etc.

position point clouds (high buildings and tree crowns) and cutting the point clouds into blocks.

First of all, we subsample each point clouds scene to reduce the number of points while maintaining the shape characteristics. A minimum distance between points is used for subsampling, leading to the distance between any two points in the point cloud after subsampling is greater than this minimum distance. A subsampled point clouds scene is a subset of the original point clouds scene. Since the LiDAR is installed on the roof of the car, and as a result the obtained road scene point clouds often include many roadside high buildings, large tree crowns, etc., we adopt appropriate height limit to cut off the point clouds which are far from the road surface. Considering that the point number of the obtained road scene data is quite different, all the road scene point clouds are cut into the regular blocks with a fixed size, each of which includes road surface, vehicles, pedestrians and objects around the road, such as road guardrails, vegetation and roadblocks.

2) Road Surface Removal: As a promising and powerful method, RANSAC is explored to find the road plane model and remove the road surface points in each point clouds block. The algorithm can fit a model to data containing outliers by means of iteration, and to a certain extent eliminate the interference of wrong samples. The road surface in each block is short in length and approximate flat plane. We use RANSAC to fit a road plane model for each point clouds block and aggregate these blocks definitively. The road surface points, which are the inliers of the plane model, are then removed. The algorithm fits the model to inliers and classifies all points within the distance threshold from the model as inliers, which allows it to find the surface points of rough and uneven roads. Road surface removal based on point clouds blocks and RANSAC enables the proposed method to adapt to rough slope roads. Considering the objective height limit of the road guardrails, we appropriately translate the road plane model vertically upwards in the residual point clouds where the road surface has been removed, and leverage it as a boundary to further filter out the undesirable point clouds outside the height range of the road guardrails. After performing the above operations on each point clouds block, the point clouds we obtained includes: the road guardrails point clouds, and the point clouds of other objects within the height range of the guardrails. These two parts of point clouds are collectively called as the candidate point clouds, on which the next step is conducted.

B. Modified DBSCAN Clustering

At this step, a modified DBSCAN clustering is applied to the candidate point clouds of each block to achieve the extraction of road guardrails.

Algorithm 1 Guardrails Extraction From MLS Point Clouds

Input:
P: road scene point clouds
$Threshold$, $Blocksize$: parameters
Output:
G: guardrails
$P.subsample()$
$P.removeByHeight(Threshold)$
$PBlocks = P.cutIntoBlock(Blocksize)$
for B in $PBlocks$ **do**
  $BPlaneModel, BRoadSurface, BResidual = B.planeFit()$
  $BCandidate = BResidual.removeByModel(BPlaneModel, Threshold)$
  $BClusters = BCandidate.project().cluster()$
  for C in $BClusters$ **do**
    if $PointNumber < Threshold$ **then**
      continue
    end if
    $FittingError = C.lineFit()$
    if $FittingError > Threshold$ **then**
      continue
    end if
    if $BoundingBoxSize < Threshold$ **then**
      continue
    end if
    if $Intensity$ not in $Threshold$ **then**
      continue
    end if
    $G = BCandidate.extract(C.index)$
  end for
end for

1) Candidate Point Clouds Clustering: To extract the road guardrails, a bird's-eye view projection strategy is proposed. Observing the candidate point clouds of each block, we find that the road guardrails can be clearly identified from a bird's-eye view, for the guardrails have thin straight line shapes and are hardly connected with other objects in the bird's-eye view, while the other objects are mostly in irregular shapes with large area, such as the vegetation in approximately rectangular shapes. The candidate point clouds in the bird's-eye view can be seen in Fig. 3. Even though the projection causes a certain loss of information, it contributes to an effective extraction of the guardrails. The fall in dimension saves the cost of time and is more computationally friendly.

After the projection is conducted in each point clouds block, we adopt DBSCAN algorithm to cluster these 2D points. Compare with traditional methods, such as region growing clustering method with difficulty in processing noise and slope point clouds data, DBSCAN is a density-based spatial clustering algorithm to cluster various shape on slope grounds and identify noise points simultaneously. These characteristics appropriate for clustering the projected candidate point clouds where the guardrails are hardly connected with other objects. The noise points are firstly filtered out by the original DBSCAN clustering and a proposed four-step screening for guardrails extraction is performed as follows.

2) Guardrails Extraction: In the final stage, we distinguish the interested clusters and achieve the extraction of road guardrails based on the after-DBSCAN point clouds.

Firstly, we exclude the clusters away from the road by limiting the number of points for each cluster. Points far away from the road are also far away from the LiDAR. The distribution of these points is sparse, and consequently the clusters have few points. Such clusters have a wide distribution, and we exclude them by setting an appropriate threshold of point number.

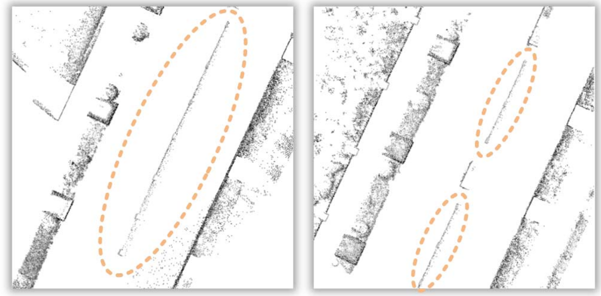

Fig. 3. Candidate point clouds in the bird's-eye view. The points of road guardrails are marked by orange dotted circles.

Secondly, the road guardrails point clouds are in thin straight line shapes after the bird's-eye view projection, so we conduct line fitting for each cluster. Based on the coordinates of all points in one cluster, we fit a straight line that accords with the least squares solution, and calculate the average error for each point. A threshold of the average fitting error is adopted to distinguish clusters of guardrails from other objects. This is based on the fact that the road guardrails of the same kind share a uniform structure and there is no big difference in the relative distance between every section of the guardrails and the LiDAR. The objects away from the LiDAR may be occluded resulting in incomplete or even broken point clouds and leading to a big loss of features. The guardrails close to the LiDAR are almost free from occlusion, and their point clouds in similar shapes should have similar error values after fitting. By the end of this step, we are able to basically sort out the clusters of road guardrails from the other ones. But there are still a small number of clusters that do not belong to guardrails class.

Thirdly, most of these misjudged clusters are in disk shapes with small area but large point density, for which the limits on the number of points and the fitting error fail to take effect on them. We use a smallest box aligned to the axis to include all the points in one cluster, and add limits on the length and width of the box to exclude these misjudged clusters. The method proves to be feasible and effective.

Finally, owing to the particularity of the roles that they play in the road environments, the guardrails are different from the common objects in their surface material, which makes their reflection intensity captured by the LiDAR different from that of the other objects. For each cluster, we calculate the average reflection intensity of all the points it contains. Based on an appropriate threshold, the clusters whose average intensity is not within the range are excluded. At this point, the clusters corresponding to the road guardrails can be well sorted out.

In summary, we first project the 3D candidate point clouds onto 2D plane in its bird's-eye view, and then use the DBSCAN algorithm to cluster the 2D points. After that, a four-step screening is performed on the obtained clusters, which includes the limits on the number of points, the fitting error, the bounding box size, and the average reflection intensity, all of which are carried out in the 2D space. And finally, we get the target guardrails point clouds in the 3D space. The clustering algorithm returns the point index for each cluster, and thereby we can easily find and extract the 3D point clouds corresponding to the 2D clusters of guardrails. The bird's-eye view projection reduces the dimension and simplifies the calculation while achieving a good extraction effect.

Fig. 4. Mobile laser scanning system for point clouds acquisition.

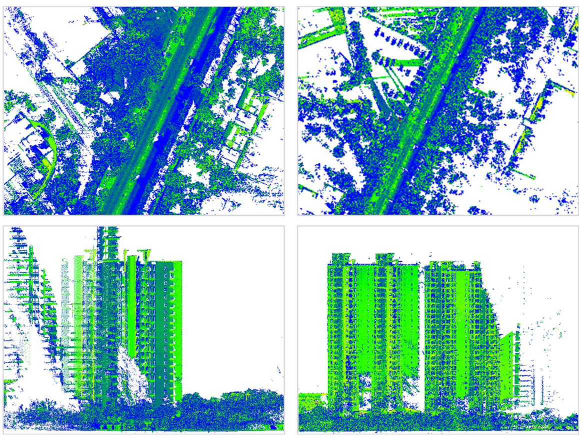

Fig. 5. Road scene point clouds. The first line shows the top view of the point clouds, and the second line shows the front view. Tall buildings and trees can be seen. Points with different reflection intensities are rendered in different colors.

III. Experiment and Discussion

The stability and capability of the proposed guardrails extraction method are evaluated using RIEGL VMX-450 MLS point clouds. The benchmark dataset is manually built for validating our method. Detailed experiments of quantitative assessment measures and algorithm complexity are provided to validate our algorithm design.

A. Data Description

To the best of our knowledge, there are no public benchmarks or datasets designed for the detection or extraction of guardrails on point clouds. We generate our own dataset by extracting the guardrails points from point clouds recorded by LiDAR sensor mounted on a moving vehicle travelling through various urban road scenes. The data is acquired in October 2019 in the dense traffic areas of International Convention and Exhibition Center and Ring Belt Road on Xiamen Island (longitude 118°04′04″E, latitude 24°26′46″N), a part of the City of Xiamen. 18 pieces of road point clouds make up the dataset, of which the size is 17.4 GB in total. As shown in Fig. 4, a RIEGL VMX-450 scanning system which integrates two RIEGL VQ-450 laser scanners, four digital cameras and inertial navigation devices is mounted on a seven-seat travelling car to capture high-density, high-precision 3D point clouds. The complete mobile laser scanning system has a high measurement speed of 1,100,000 points per second, a high scanning speed of 400 lines per second and an effective range of up to 800 meters.

It is necessary to conduct data preprocessing on the original road scene point clouds to facilitate the following operations and reduce the computational complexity. Fig. 5 shows the original road scene point clouds.

B. Ground Truth and Samples

We test our method using our manual dataset to evaluate the performance of our proposed algorithm for extracting 3D guardrails from point clouds. To obtain the ground truth, we manually segment the guardrails points in each point clouds scene and save all the guardrails belonging to the same road scene as one point clouds file, based on which we calculate the assessment metrics.

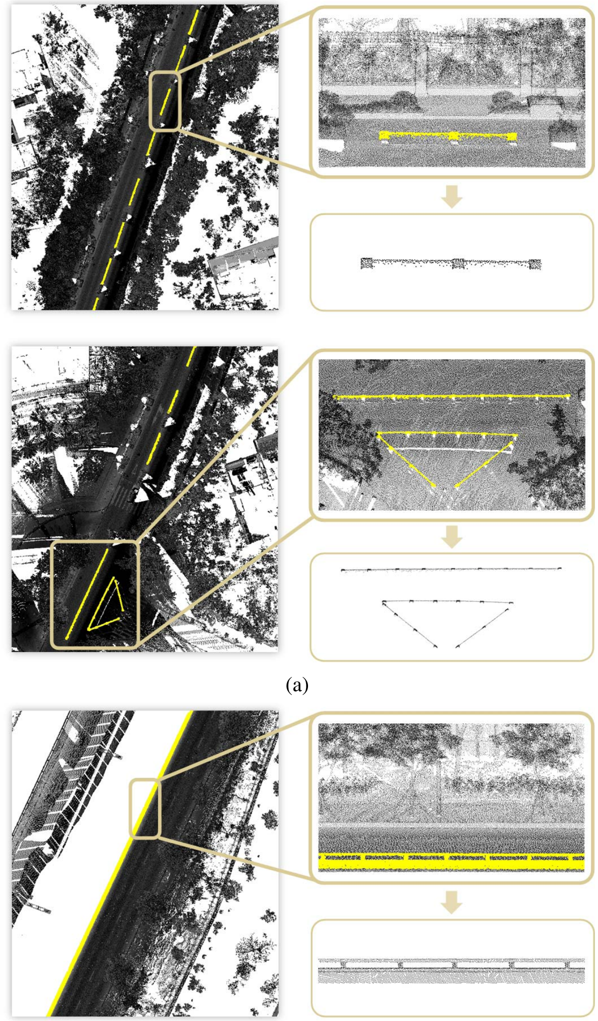

(a)

(b)

Fig. 6. Extraction results of road guardrails: (a) lane-separating guardrails, (b) anti-fall guardrails on the elevated road. The extracted guardrails point clouds are highlighted in yellow.

The manual dataset has a total of 18 pieces of road point clouds, of which 15 are ordinary urban roads including lane-separating guardrails and the other 3 are elevated roads including anti-fall guardrails. Each road scene contains an average of 30 million points and has an average road length of 450 m. We obtain 18 ground truth guardrails point clouds in total. The average size for one lane-separating guardrails sample is 0.18 MB, and 9 MB for one anti-fall guardrails sample.

C. Guardrails Extraction Result

The adjustment of the parameters for the proposed algorithm is intuitive. Most of the parameters are distance parameters, such as the maximum height of the near-road point clouds in preprocessing and the distance threshold for inliers in RANSAC. The experiment results prove the effectiveness of the algorithm, as shown in Fig. 6. Two types of guardrails, lane-separating guardrails (Fig. 6(a)) and anti-fall guardrails (Fig. 6(b)), are extracted. In Fig. 6(a), we illustrate two situations in which the lane-separating guardrails are placed

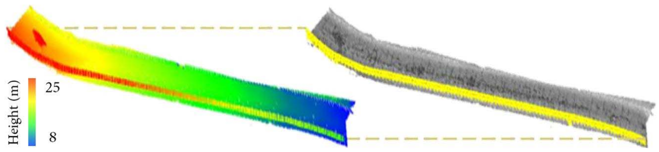

Fig. 7. Extraction result of guardrails on slope road.

differently: the lane-separating guardrails made of poles and concrete blocks are placed in line in the middle of the road (top), and placed in the triangle to mark non-travellable areas (bottom). In the first situation, 8 guardrails placed in line are extracted in a 200-meter scene. In the second situation, a group of guardrails placed in the triangle is extracted along with 4 guardrails placed in line. Fig. 6(b) shows the extraction results of the anti-fall guardrails, which contain beams, columns and a continuous concrete wall installed on one or both sides of the elevated roads. The continuous structure of the anti-fall guardrails is correctly extracted and the concrete wall generates a large number of points. The proposed algorithm takes advantage of the distribution of the points and performs satisfactorily for these two types of guardrails.

To verify the adaptability of our method for slope roads, we extract guardrails of a 100-meter slope road with an inclination angle of 10°. As shown in Fig. 7, the guardrails on slope are correctly and qualitatively extracted. The original data on the left is rendered based on height, and the yellow areas on the right figure are the guardrails extraction results.

Comparative experiment on region growing clustering methods and our proposed method were conducted for 3D clustering on the candidate point clouds. Fig. 8 shows that clustering results of two methods. It illustrated that the DBSCAN method (Fig. 8 (b)) achieve the accurate performance he best performance, while region growing clustering results (Fig. 8 (a)) more structures but with trivial over-segmentation of the red box on the guardrail parts.

D. Quantitative Assessment Measures

We calculate the assessment metrics based on each piece of road point clouds, where the precision and recall are respectively defined as (1) and (2), and the F_1-measure is adopted to comprehensively evaluate the performance as (3).

$$PRE = \frac{N_{TP}}{N_{TP} + N_{FP}} \tag{1}$$

$$REC = \frac{N_{TP}}{N_{TP} + N_{FN}} \tag{2}$$

$$F_1 - Measure = 2 \times \frac{PRE \times REC}{PRE + REC} \tag{3}$$

N_{TP} is the number for the correct guardrails points extracted; N_{FP} is the number for the wrong points extracted; N_{FN} is the number for the guardrails points failed to extract.

The assessment results are shown in Table I. The proposed method was compared with the algorithm proposed by [12] based on the same dataset described in Section III-A. Our proposed method performed efficiently and achieved a better accuracy rate than [12], especially in extracting the lane-separating guardrails. The proposed method got an F_1 score of 93.2%, compared with 77.9% acquired by [12] for the lane-separating guardrails. And for the anti-fall guardrails, two methods obtained similar extraction effects with an F_1 score of 92.7% by ours and 91.9% by [12]. The results show that our method has great advantages when the length of the single guardrails part is short and there are obstacles between the guardrails, such as the lane-separating guardrails which are placed alternately with bushes. And when the guardrails have a continuous structure like the anti-fall guardrails, the proposed method also performs well. Our method got

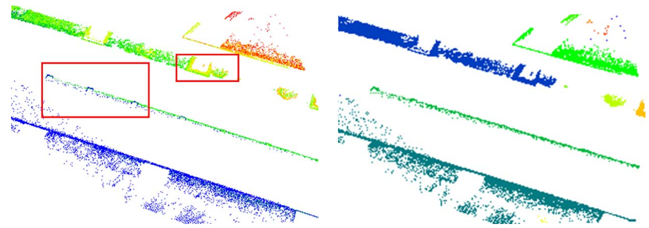

(a) (b)

Fig. 8. Clustering comparison results.

TABLE I

ASSESSMENT RESULTS

Guardrails Type	Method	Precision (%)	Recall (%)	F_1-Measure (%)
Lane-Separating Guardrails	Method [12]	92.5	67.3	77.9
	Ours	**97.2**	**89.6**	**93.2**
Anti-Fall Guardrails	Method [12]	95.9	88.3	91.9
	Ours	**96.4**	**89.2**	**92.7**
Both Guardrails	Method [12]	94.2	77.8	84.9
	Ours	**96.8**	**89.4**	**93.0**

an overall F_1 score of 93.0% for both types of guardrails, 8.1% higher than [12]. Moreover, the precisions we got have higher values than the recalls, with a difference of 7.6% for the lane-separating guardrails and 7.2% for the anti-fall guardrails, which is mainly due to the strict screening conditions we set based on the characteristics of the guardrails. However, our method caused a small number of failure cases. The main reason for the failure of extraction is that some guardrails are covered by the bushes or the guardrails are too short in length.

E. Complexity Analysis

All experiments were performed on a 64-bit ubuntu 16.04 LTS system with Intel Core i5-8400 2.80 GHz × 6 CPU and 8.00 GB RAM. For a road point clouds scene with an average of 30 million points and a 450 m length, the average time consumed by the proposed algorithm was 11 seconds, excluding the time spent on data loading and preprocessing, while [12] took 19 seconds and region growing-based method took 20 seconds under the same data and operating environments. Of the total 11 seconds, finding and removing the road surface points took an average of 7 seconds, and the subsequent steps took an average of 4 seconds. The total time consumed by the extraction algorithm for the entire dataset with 540 million points and 8100 m length was within 200 seconds.

IV. CONCLUSION

In this paper, we proposed a novel 3D guardrails extraction algorithm for transportation-related applications. By leveraging a multi-level filtering strategy, the proposed method rapidly handled large volumes of MLS point clouds toward 3D guardrails extraction. Our rapid extraction algorithm was successfully applied to the 3D MLS dataset. For a point clouds dataset containing about 540 million points and a road length of approximately 8100 m, the total computing time for extracting 3D guardrails is within 200 seconds. Qualitative and quantitative evaluations demonstrated that our proposed method achieved a promising performance. Our method achieves high precisions of 97.2% and 96.4% for two types of guardrails respectively, which benefits from the strict screening conditions based on the characteristics of the guardrails. Comparative studies demonstrated that our proposed algorithm outperforms the state-of-the-art algorithm in extracting 3D guardrails. Therefore, we provide a feasible and promising solution to the rapid extraction of urban guardrails using MLS systems. Future extensions will be oriented to automate the extraction process and explore methods based on deep learning for smarter operations and better performance.

REFERENCES

[1] Y. Xu *et al.*, "Classification of LiDAR point clouds using supervoxel-based detrended feature and perception-weighted graphical model," *IEEE J. Sel. Topics Appl. Earth Observ. Remote Sens.*, vol. 13, pp. 72–88, 2020.

[2] Z. Yan, T. Duckett, and N. Bellotto, "Online learning for 3D LiDAR-based human detection: Experimental analysis of point cloud clustering and classification methods," *Auto. Robots*, vol. 44, no. 2, pp. 147–164, Jan. 2020.

[3] R. Huang, Y. Xu, D. Hong, W. Yao, P. Ghamisi, and U. Stilla, "Deep point embedding for urban classification using ALS point clouds: A new perspective from local to global," *ISPRS J. Photogramm. Remote Sens.*, vol. 163, pp. 62–81, May 2020.

[4] C. Wen *et al.*, "Spatial-related traffic sign inspection for inventory purposes using mobile laser scanning data," *IEEE Trans. Intell. Transp. Syst.*, vol. 17, no. 1, pp. 27–37, Jan. 2016.

[5] D. R. Bruno, D. O. Sales, J. Amaro, and F. S. Osorio, "Analysis and fusion of 2D and 3D images applied for detection and recognition of traffic signs using a new method of features extraction in conjunction with deep learning," in *Proc. Int. Joint Conf. Neural Netw. (IJCNN)*, Jul. 2018, pp. 1–8.

[6] F. Wu *et al.*, "Rapid localization and extraction of street light poles in mobile LiDAR point clouds: A supervoxel-based approach," *IEEE Trans. Intell. Transp. Syst.*, vol. 18, no. 2, pp. 292–305, Feb. 2017.

[7] H. Guan, Y. Yu, J. Li, and P. Liu, "Pole-like road object detection in mobile LiDAR data via supervoxel and bag-of-contextual-visual-words representation," *IEEE Geosci. Remote Sens. Lett.*, vol. 13, no. 4, pp. 520–524, Apr. 2016.

[8] Y. Yu, J. Li, H. Guan, and C. Wang, "Automated detection of three-dimensional cars in mobile laser scanning point clouds using DBM-Hough-forests," *IEEE Trans. Geosci. Remote Sens.*, vol. 54, no. 7, pp. 4130–4142, Jul. 2016.

[9] J. Huang and S. You, "Vehicle detection in urban point clouds with orthogonal-view convolutional neural network," in *Proc. IEEE Int. Conf. Image Process. (ICIP)*, Sep. 2016, pp. 2593–2597.

[10] T. Scharwachter, M. Schuler, and U. Franke, "Visual guard rail detection for advanced highway assistance systems," in *Proc. IEEE Intell. Vehicles Symp.*, Jun. 2014, pp. 900–905.

[11] A. Seibert, M. Hahnel, A. Tewes, and R. Rojas, "Camera based detection and classification of soft shoulders, curbs and guardrails," in *Proc. IEEE Intell. Vehicles Symp. (IV)*, Jun. 2013, pp. 853–858.

[12] H. Masuda, S. Oguri, and J. He, "Shape reconstruction of poles and plates from vehicle-based laser scanning data," in *Proc. Inf. Symp. Mobile Mapping Technol.*, vol. 201, Jan. 2013.

[13] Y. Jiang, B. He, L. Liu, R. Ai, and X. Lang, "Effective and robust corrugated beam guardrail detection based on mobile laser scanning data," in *Proc. IEEE 19th Int. Conf. Intell. Transp. Syst. (ITSC)*, Nov. 2016, pp. 1540–1545.

[14] H. Zhu and B. Guo, "A beam guardrail detection algorithm using LiDAR for intelligent vehicle," in *Proc. IEEE 8th Annu. Int. Conf. CYBER Technol. Autom., Control, Intell. Syst. (CYBER)*, Jul. 2018, pp. 1398–1402.

[15] H. Matsumoto, Y. Mori, and H. Masuda, "Extraction and shape reconstruction of guardrails using mobile mapping data," *ISPRS-Int. Arch. Photogramm., Remote Sens. Spatial Inf. Sci.*, vol. XLII-2/W13, pp. 1061–1068, Jun. 2019.

[16] M. Ester, H. P. Kriegel, J. Sander, and X. Xu, "A density-based algorithm for discovering clusters in large spatial databases with noise," in *Proc. 2nd Int. Conf. Knowl. Discovery Data Mining*, vol. 96, Aug. 1996, pp. 226–231.

[17] M. A. Fischler and R. C. Bolles, "Random sample consensus: A paradigm for model fitting with applications to image analysis and automated cartography," *Commun. ACM*, vol. 24, no. 6, pp. 381–395, Jun. 1981.